

⁴J. E. Eby, K. J. Teegarden, and D. B. Dutton, *Phys. Rev.* **116**, 1099 (1959).

⁵H. B. DeVore, *Phys. Rev.* **102**, 86 (1956).

⁶F. Urbach, *Phys. Rev.* **92**, 1324 (1953).

⁷D. L. Dexter, *Nuovo Cimento* **7**, 245 (1958).

⁸W. Martienssen, *Phys. Chem. Solids* **2**, 257 (1957).

⁹G. R. Huggett and K. Teegarden, *Phys. Rev.* **141**, 797 (1966).

¹⁰M. Sydor, *Phys. Rev.* **163**, 873 (1967).

¹¹M. Sydor, *Phys. Rev.* **183**, 846 (1969).

PHYSICAL REVIEW B

VOLUME 5, NUMBER 2

15 JANUARY 1972

Noncollinear Attenuation of Transverse Acoustic Waves in Al_2O_3 †

R. C. Purdom*

Department of Physics, Purdue University, Lafayette, Indiana 47907
and Department of Physics and Mathematics, Kentucky Wesleyan College, Owensboro, Kentucky 42301

and

E. W. Prohofskey

Department of Physics, Purdue University, Lafayette, Indiana 47907

(Received 28 July 1971)

For transverse waves propagated along an even-fold axis, the phonon-phonon coupling parameters are zero for collinear interactions. This necessitates a consideration of the angular dependence of the coupling parameter. The angle at which these parameters peak affects the minimum energy deficit possible on interactions. A calculation including both the angular dependence of the coupling parameters and the uncertainty of phonon energy due to thermal-phonon lifetimes is done for the case of Al_2O_3 along the a axis. The calculated attenuation fits the experimentally observed attenuation.

I. INTRODUCTION

The agreement of theoretical calculations of ultrasonic attenuation in insulators at low temperatures with experimental observation has greatly improved since the uncertainty in energy of the thermal phonons has been included.^{1,2} This uncertainty in energy arises because of the extremely short lifetime of thermal phonons due to their interactions with other thermal phonons and/or defects. The uncertainty in energy allows processes to occur which are not included in the Golden Rule calculation of Landau and Rumer.³

Although these non-energy-conserving processes are reduced in probability over strictly conserving processes, in many materials no conserving processes are possible, and in addition there are so many such nonconserving processes possible that their total effect on the attenuation can be the greater. In such cases one can get attenuation considerably different than that predicted by Landau and Rumer.

In this paper, we consider the measurements by de Klerk⁴ of the attenuation along an even-fold axis in Al_2O_3 . He has found the attenuation to have a T^9 , T^7 , and T^4 temperature dependence for the longitudinal, fast transverse, and slow transverse waves, respectively, at lowest temperatures. The first two of these dependences are clearly in dis-

agreement with the predictions of the Landau-Rumer theory. We will consider the attenuation of the transverse waves in detail in Secs. III and IV.

The equation for calculating the three-phonon interaction in the presence of finite lifetimes developed by Simons² replaces the energy-conserving δ function by

$$\langle \sin \Omega t / \Omega \rangle = \int_0^\infty e^{-t/\tau} \sin \Omega t / \Omega \int_0^\infty e^{-t'/\tau} dt' \quad (1)$$

$$= \frac{\tau}{1 + \Omega^2 \tau^2} \quad (2)$$

Here τ is the thermal-phonon lifetime and Ω is the energy deficit

$$\Omega = \omega_2 - \omega_1 - \omega \quad (3)$$

where ω_2 is the frequency of the final thermal phonon, ω_1 the frequency of initial thermal phonon, and ω the frequency of the acoustic wave. The integral in the numerator allows for the decay of the coherent state (through other channels) and reduces the interaction considered. The denominator corrects for the fact that the thermal phonons are not depopulated by the thermalizing collisions. It essentially normalizes the population of the thermal phonons to their equilibrium value. The range of validity of Eq. (1) has been investigated by Leggett and ter Haar.⁵

One can consider Eq. (2) to be a weighting func-

tion for the transition probability due to energy-conservation effects. This function is shown in Fig. 1. Processes in which energy is strictly conserved would be those at $\Omega=0$. Processes which do not strictly conserve energy but are allowed within the uncertainty principle fall within the central maximum. The width of this maximum is controlled by the denominator of Eq. (2). The half-width occurs for $\Omega\tau=1$. This width is therefore τ^{-1} and these processes are quasilowed in the usual sense of the uncertainty relation. There is also a finite probability for interactions to occur for very large energy defects $\Omega\tau > 1$, although this probability falls off as Ω^{-2} . For the sake of clarity in the following discussion, we will refer to these three types of processes: allowed, quasilowed (i. e., those in the central maximum), and unallowed (i. e., those out on the tail of the probability distribution).

The total attenuation comes from integrating over all possible processes which contribute. This includes integrating Eq. (2) over energy or Ω . This function is normalized to unity just as the δ function is for $\tau=\infty$, as in the Landau-Rumer case. If all Ω processes are allowed by the dispersion relations of the material, one should get the same answer as Landau and Rumer and a T^4 dependence. This can be understood physically in the following way. The largest contribution to the integral of Eq. (2) comes from the central maximum. For finite lifetime the probability of each process is reduced by τ due to the competition of thermal processes. However, the quasilowed processes extend over a range in Ω of τ^{-1} due to lifetime broadening of the levels. These two effects tend to cancel leaving the area of the maximum roughly constant.

In some solids the dispersion relations may be such that no processes exist in which the energy can be conserved. Also, it may be that the coupling parameter for energy-conserving processes may be zero. In either case, no energy-conserving processes can occur. This would make other factors in the scattering integrals zero for some range of values of Ω near $\Omega=0$. A first approximation of the effect of these selection rules would be to exclude regions in the integral over Ω of Eq. (2). Consider excluding all $|\Omega| < \Omega_0$, where Ω_0 is the smallest energy defect for which collisions are possible. If $\Omega_0\tau \ll 1$, i. e., falls well within the central maximum, many quasilowed processes can occur. Since the allowed and quasilowed processes for $\Omega\tau \ll 1$ have the same probability (the curve of Fig. 1 is relatively flat at $\Omega=0$), the exclusion of the small region in the central maximum does not alter the total attenuation very much.

On the other hand, if $\Omega_0\tau \gg 1$, the entire central maximum is excluded and only processes on the

probability tail can take place. In this region Eq. (2) can be approximated by

$$\langle \sin \Omega t / \Omega \rangle \approx 1 / \pi \Omega^2 \tau \quad (4)$$

and the integral will be proportional to $1/\Omega_0\tau$.

For $\Omega_0\tau \ll 1$ the result is very close to the Landau-Rumer result which assumes energy conservation, and the temperature dependence in normal materials should go as T^4 . For $\Omega_0\tau \ll 1$ the extra factor τ^{-1} appears, and in the final result for the attenuation, temperature dependence should go as $T^4 (1/\tau) \propto T^9$, neglecting any temperature dependence of Ω_0 . For $\Omega_0\tau \approx 1$ the attenuation is from unallowed transitions as well as from some quasilowed transitions, and the temperature dependence of this mixed case should be between the two limits of T^4 and T^9 .

In view of the above arguments, the measurements by de Klerk on Al_2O_3 along the a axis is particularly striking; see Fig. 2. The slow transverse wave is seen to go as T^4 for all temperatures, the fast transverse wave as T^7 for lowest temperatures, and the longitudinal wave as T^9 for lowest temperatures. At higher temperatures all seem to vary as T^4 . This spans the range expected on the basis of the above discussion. The shift of the fast transverse and longitudinal waves to T^4 dependence at higher temperatures can be explained on the basis of a decrease in $\Omega_0\tau$ at higher temperatures. As τ decreases, the central maximum increases; see Fig. 1. An energy deficit Ω_0 which is outside or on the edge of the central maximum will be well inside the central maximum at higher T and the quasilowed processes will dominate.

II. DISPERSION RELATIONS AND ENERGY DEFICIT IN Al_2O_3

The energy deficit

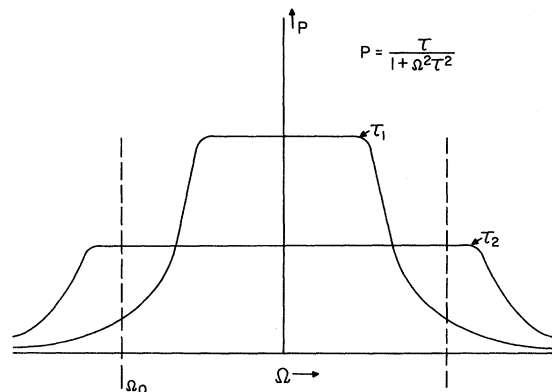


FIG. 1. Probability of a particular transition as a function of its energy deficit for two thermal-phonon lifetimes. The shorter lifetime curve is lower and broader. The area under the curves is conserved. The dashed line at deficit $\Omega = \Omega_0$ is a particular interaction which is on the probability tail for long lifetimes but is in the central maximum for short lifetimes.

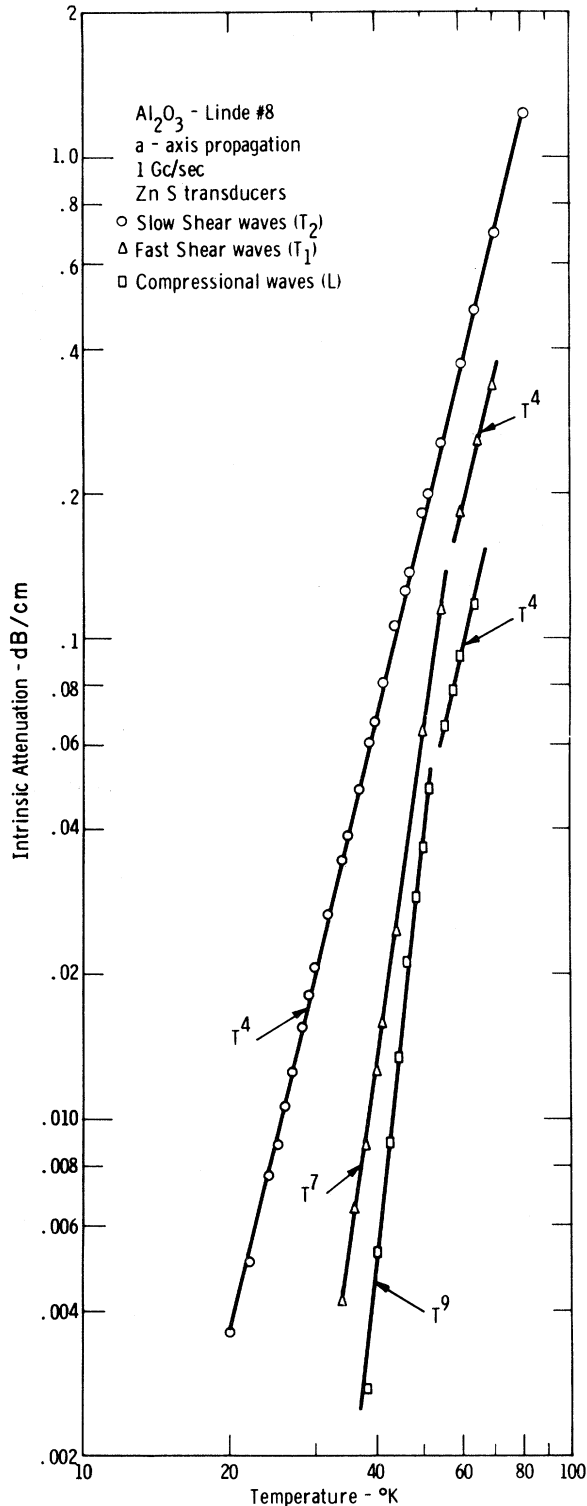


FIG. 2. Attenuation along the a axis in Al_2O_3 from Ref. 4 (reprinted with permission).

$$\Omega = \omega_2 - \omega_1 - \omega \quad (5)$$

can be approximated where the energy of the acous-

tic wave ω is small compared to thermal waves ω_1, ω_2 :

$$\Omega \approx \nabla_k \omega_{\text{th}} \cdot \vec{k} - \omega = \omega(\beta \cos \theta - 1), \quad (6)$$

$$\beta = \frac{v_{\text{gth}}}{v_{\text{pa}}}, \quad (7)$$

where $\nabla_k \omega_{\text{th}}$ is the gradient in k space of the thermal phonons, v_{gth} the thermal group velocity, v_{pa} the acoustic phase velocity, and k the acoustic-phonon wave vector. The angle θ is essentially the angle between the acoustic phonon and the direction of the thermal phonons as $k \ll k_1, k_2$ and $k_1 + k = k_2$. The assumption has been made that ω_1 and ω_2 lie on the same phonon branch as $\omega \ll \omega_1, \omega_2$.

For the longitudinal wave in Al_2O_3 , v_{pa} is by far the largest velocity in the crystal, and since $\cos \theta \leq 1$,

$$(v_{\text{gth}}/v_{\text{pa}}) \cos \theta < 1 \quad (8)$$

and Ω is always large. The thermal-phonon lifetimes have been measured to be proportional to T^{-5} by von Gutfeld and Nethercot.⁶ One then expects a large temperature dependence for interactions with any branch, and certainly a T^9 dependence for attenuation dominated by interactions with fast or slow transverse thermal phonons.⁷ This situation is shown schematically for isotropic-phonon velocities in part (a) of Fig. 3.

In the case of the fast transverse wave one would normally expect that energy-conserving transitions could occur in which the two thermal phonons are longitudinal. In this case β would be greater than 1.

This would give rise to standard Landau-Rumer attenuation and a T^4 dependence would be expected. A calculation of this mechanism for the attenuation turns out to be too small to explain de Klerk's results. The reason is that the longitudinal branch in Al_2O_3 is much higher in energy than the other acoustic modes. Thus the k vector is small for those thermally activated phonons. The small k vector implies a small density of states, and few phonons of this branch are available for interaction. The energy-conserving process then does not dominate the attenuation.

Another possibility is interaction with fast transverse waves. The dispersion is not great and for a fast transverse wave scattering off a fast transverse thermal phonon the crucial parameter $\beta \approx 1$. The deficit Ω can be zero for $\theta = 0$, i.e., all the phonons involved are collinear. This case corresponds to part (b) of Fig. 3. For the interaction of fast transverse with slow transverse thermal phonons, $\beta < 1$ and the energy deficit would be very large reducing the strength of this interaction. This, as in the longitudinal case, would correspond to part (c) of Fig. 3.

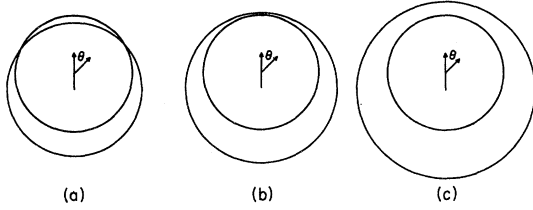


FIG. 3. Two-dimensional plot to determine energy and momentum conservation for an acoustic and two thermal phonons. The smaller circle is the constant energy surface ω_1 (i. e., all k_1 such that $\omega = \omega_1$). The large circle is the constant energy surface ω_2 chosen such that $\omega_2 = \omega_1 + \omega$, where ω_2 is the final thermal, ω_1 the initial thermal, and ω the acoustic phonon energy. The center of the small circle is displaced from the center of the large circle by k , the acoustic-phonon wave vector. Therefore an intersection of ω_1 and ω_2 guarantees the simultaneous satisfying of $\omega_1 + \omega = \omega_2$ and $k_1 + k = k_2$. Parts (a), (b), and (c) represent cases where the ratios of β (thermal-group to acoustic-phase velocities) are $\beta > 1$, $\beta = 1$, and $\beta < 1$, respectively.

In Al_2O_3 , however, along the a axis, the coupling constant is zero for collinear transverse waves. Thus no processes for $\theta = 0$, or therefore $\Omega = 0$, occur. In Sec. III it is shown that the coupling constant peaks for an angle θ of about 45° . As seen in (b) of Fig. 3 this causes a nonzero Ω_0 . For the particular values of τ in Al_2O_3 at the appropriate temperatures, the scattering at $\theta = 45^\circ$ has $\Omega_0\tau \approx 1$ and the detailed calculation in Sec. IV fits the T^7 dependence observed. If $\theta = 0^\circ$ scattering were allowed then $\Omega_0\tau \ll 1$. A similar case of collinear scattering has been calculated by Maris⁸ and the result is a T^4 temperature dependence. If the third-order elastic constant has peaked at $\theta = 90^\circ$ the value of $\Omega_0\tau$ would have been greater [see part (b), Fig. 3], and the temperature dependence would be T^9 . Shiren⁹ has calculated the ultrasonic attenuation for such a large-angle noncollinear scattering case.

The slow transverse wave has low phase velocity and can conserve energy in collisions with thermal phonons from both the fast transverse and longitudinal branches. Such collisions are diagrammed in part (a) of Fig. 3. The lower v_{th} of the fast transverse waves compared to the longitudinal waves gives rise to a greater density of states for the thermally activated phonons. This gives rise, as shown in Sec. IV, to a v_{th}^{-10} dependence. The ratio of longitudinal to fast transverse phonons in Al_2O_3 along the a axis is $\frac{5}{3}$. This greatly favors damping by the fast transverse wave.

III. ANGULAR DEPENDENCE OF THE THIRD-ORDER ELASTIC CONSTANTS FOR TRANSVERSE WAVES

We use the third-order elastic constants recently measured for Al_2O_3 by Hankey and Schuele¹⁰ to

make an approximate calculation of the true coupling parameter.

The normal coordinate system notation for Al_2O_3 is that the a axis is designated as the x_1 direction, the trigonal c axis as the x_3 direction, and the axis perpendicular to the $x_1 - x_3$ plane as the x_2 direction. A fast transverse wave propagating in the a or x_1 direction would be polarized in the x_2 direction.

We calculate the approximate coupling parameter for the interaction of fast transverse phonons with \vec{k}_1 in the $x_1 - x_3$ plane by assuming $\vec{\epsilon}_1$, the polarization vector, is always in the x_2 direction, and the parameter obtained is¹¹

$$\begin{aligned} A_{t.t.+t.t.-t.t.}(x_1-x_3 \text{ plane of } \text{Al}_2\text{O}_3) \\ &= 2(C_{466} + 3C_{14}) \sin\theta \cos\theta \\ &= -2.2 \times 10^{12} \sin\theta \cos\theta \text{ dyne/cm}^2 \quad (9) \end{aligned}$$

We calculate the approximate coupling parameter for the interaction of fast transverse phonons with \vec{k}_1 in the $x_1 - x_2$ plane by assuming that $\vec{\epsilon}$ is also in the $x_1 - x_2$ plane and perpendicular to \vec{k}_1 . This coupling parameter is given by Eq. (10):

$$\begin{aligned} A_{t.t.+t.t.-t.t.}(x_1-x_2 \text{ plane of } \text{Al}_2\text{O}_3) \\ &= 2(C_{266} - C_{166}) \sin\theta \cos\theta (\cos^2\theta - \sin^2\theta) \\ &= 1.3 \times 10^{13} \sin\theta \cos\theta (\cos^2\theta - \sin^2\theta) \text{ dyne/cm}^2 \quad (10) \end{aligned}$$

The square of the coupling parameters enters into the attenuation, and in Fig. 4 we plot the square of Eq. (9) (dotted line) and the square of Eq. (10) (solid line).

To calculate the attenuation one must integrate not only over symmetry directions but over all directions about the a axis. This was handled by assuming a simplified form for the coupling coefficient.

This form is considered independent of angle φ and was used in the actual calculation of Sec. IV. This form is

$$A_{t+t-t} = \bar{A}_{t+t-t}(\text{noncollinear}) \sin\theta \cos\theta \quad (11)$$

The best value of \bar{A}_{t+t-t} from a fit of the experimental data is $\bar{A}_{t+t-t} = 8.3 \times 10^{12}$ dyne/cm². Equation (11) squared with this value is plotted as the dashed line in Fig. 4.

To see how the various equations for coupling constant effect the attenuation, we plot the squares of Eqs. (9)–(11) weighted by the probability of transition due to energy deficit, Eq. (2), as a function of $\cos\theta$ in Fig. 5. Expression (9) corresponds to the dotted line, expression (10) to the solid line, and expression (11) to the dashed line. The energy-deficit weighting function used a value of $\omega\tau \approx 50$ which is appropriate to the case of Al_2O_3 at the temperatures of de Klerk's⁴ experi-

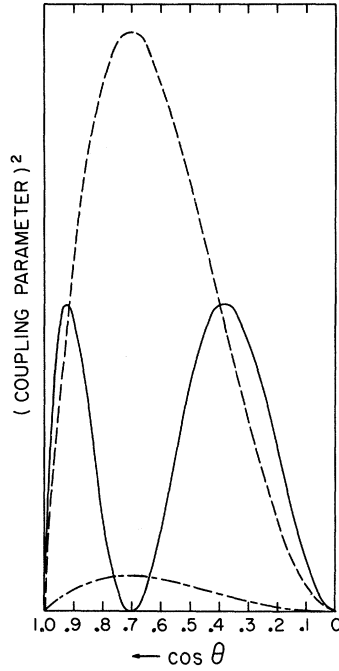


FIG. 4. Angular dependence of the square of the coupling parameter for various models. The dashed line represents the approximate model used in further calculations. The dotted line is appropriate to waves polarized in the x_2 direction. The solid line is appropriate to waves polarized in the x_1-x_2 plane perpendicular to the k vector.

ment. The lifetime was taken from von Gutfeld and Nethercot.⁶

As can be seen the assumed value falls between the values along the two symmetry planes and should therefore be a fair extrapolation of the coupling parameter for all values of φ between the two planes. This inference is further strengthened by the fact that if one were to use a coupling parameter with functional dependence of θ as in Eq. (10) the resultant temperature dependence would be the same as that for Eq. (11). The magnitude would scale with the choice of the constant $\bar{A}_{t \rightarrow t \rightarrow t}$. This has been calculated in Ref. 10. The reason for this is that the T dependence for a situation as this [i. e., part (b) of Fig. 3] is determined by the θ dependence of the weighted coupling parameter. It can be seen in Fig. 5 that all the forms peak in the same region in $\cos \theta$ and merely differ in magnitude.

The same calculation can be made for the slow transverse wave. A slow transverse wave propagating in the x_1 direction is polarized in the x_3 direction in Al_2O_3 . Therefore the approximate coupling parameter for \vec{k}_1 in the x_1-x_3 plane, assuming $\vec{\epsilon}_1$ is always in the x_2 direction, is given by

$$\begin{aligned} A_{s.t.\rightarrow t.t.\rightarrow t.t.}(x_1-x_3 \text{ plane of } \text{Al}_2\text{O}_3) \\ = 2(C_{456} + C_{44}) \sin \theta \cos \theta \\ = -5.6 \times 10^{12} \sin \theta \cos \theta \text{ dyne/cm}^2. \end{aligned} \quad (12)$$

For \vec{k}_1 and $\vec{\epsilon}_1$ in the x_1-x_2 plane, and $\vec{\epsilon}_1$ perpendicular to \vec{k}_1 , the approximate coupling parameter is

$$\begin{aligned} A_{s.t.\rightarrow t.t.\rightarrow t.t.}(x_1-x_2 \text{ plane of } \text{Al}_2\text{O}_3) \\ = 2C_{14}(\sin \theta \cos \theta) - 4C_{124}(\sin \theta \cos \theta) \\ \times (\cos^2 \theta - \sin^2 \theta) \\ = -2.0 \times 10^{12} \sin \theta \cos \theta \\ \times (\sin^2 \theta - 0.54 \cos^2 \theta) \text{ dyne/cm}^2. \end{aligned} \quad (13)$$

Again this is simplified to the same form as in the fast transverse case with a fitted parameter:

$$\bar{A}_{s.t.\rightarrow t.t.\rightarrow t.t.} = 3.6 \times 10^{12} \text{ dyne/cm}^2.$$

IV. NONCOLLINEAR ATTENUATION OF TRANSVERSE WAVES

The expression for the attenuation of ultrasound as given by Landau and Rumer after summation over the final thermal phonon states is³

$$\begin{aligned} \alpha = \frac{4 \cdot 34 \hbar \omega^2}{32 \pi^2 \rho^3 v^3} \iiint \frac{A_p^2 k_1^4}{\omega_1^2} \frac{\partial N_1}{\partial \omega_1} \delta(\omega_2 - \omega_1 - \omega) \\ \times k_1^2 dk_1 \sin \theta d\theta d\varphi. \end{aligned} \quad (14)$$

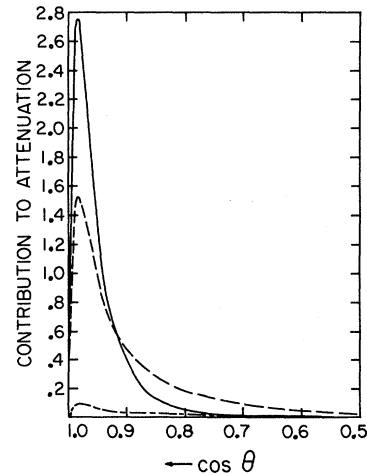


FIG. 5. Relative contribution to the attenuation as a function of angle for the different coupling parameter models. The dashed line is the approximation used in the later calculation. The long-dash short-dash line is for waves polarized in the x_2 direction. The solid line is for waves polarized in the x_1-x_2 plane perpendicular to the k vector. A representative value $\omega\tau=50$ was used in the calculation.

To take the energy uncertainty into account, one must replace the δ function by the Lorentzian of Eq. (2).² Substituting Eqs. (11) and (2) into (14), we get

$$\alpha = \frac{4.34\pi\hbar\omega}{120\rho^3v_3^3v_1^7} \left(\frac{k_B T}{\hbar}\right)^4$$

$$\alpha = \frac{4.34\pi\hbar\omega\bar{A}_{s,t.,f.,t.,-f.,t.}^2(\text{noncollinear})}{60\rho^3v_3^3v_1^7} \left(\frac{k_B T}{\hbar}\right)^4 \left\{ \frac{\pi}{\beta^3} \left(1 - \frac{1}{\beta^2}\right) [\arctan(1+\beta)\omega\tau - \arctan(1-\beta)\omega\tau] + \frac{\pi}{\omega\tau\beta^2} \left[\frac{4}{3} - \frac{6}{\beta^2} + \left(\frac{2}{\beta^3} - \frac{1}{\beta}\right) \left(\ln[1 + [\omega\tau(1+\beta)]^2] - \ln[1 + [\omega\tau(1-\beta)]^2] \right) \right] \right\}. \quad (16)$$

A. Fast Transverse Waves

For fast transverse waves interacting with fast transverse thermal phonons at low temperatures, the group velocity v_{gth} and phase velocity v_{pa} are about equal. The ratio of these velocities is $\beta \approx 1$. Therefore, collisions could be close to energy conserving at $\theta = 0^\circ$ in Eq. (6). In a solid with isotropic phonon velocities this implies

$$\Omega(\theta=0)\tau < 1 \quad \text{or} \quad |\omega(\beta-1)\tau| < 1. \quad (17)$$

In this limit, Eq. (16) reduces to

$$\alpha = \frac{4.34\pi^2\hbar\bar{A}_{s,t.,f.,t.,-f.,t.}^2(\text{noncollinear})}{60\rho^3v_3^3v_1^9} \times \left(\frac{k_B T}{\hbar}\right)^4 \frac{1}{\tau} \left[2\ln(2\omega\tau) - \frac{14}{3} \right]. \quad (18)$$

One sees the expected T^4/τ temperature behavior modified by the expression in parentheses. For values of τ in Al_2O_3 taken from heat-pulse measurements by von Gutfeld and Nethercot,⁶ Eq. (18) can be fit to the data of de Klerk. This is shown in Fig. 6. The value of $\bar{A}_{s,t.,f.,t.,-f.,t.}^2$ for the best fit which is shown is $8.0 \times 10^{25} \text{ dyne}^2/\text{cm}^4$.

B. Attenuation of Slow Transverse Waves

For slow transverse waves interacting with fast transverse thermal phonons, $v_{pa} < v_{gth}$ and $\beta > 1$. In this limit, Eq. (16) reduces to

$$\alpha = \frac{4.34\pi^3\hbar\omega\bar{A}_{s,t.,f.,t.,-f.,t.}^2(\text{noncollinear})}{60\rho^3v_1^{10}} \times \left(1 - \frac{1}{\beta^2}\right) \left(\frac{k_B T}{\hbar}\right)^4. \quad (19)$$

This expression varies as T^4 , and is identical to the Landau-Rumer expression except for the coupling parameter, and the dependence on the fast transverse velocity instead of the longitudinal phonon velocity. The $(1/v_1)^{10}$ dependence of the

$$\times \iint \frac{\omega\tau\bar{A}_{s,t.,f.,t.,-f.,t.}^2(\text{noncollinear})d(\cos\theta)d\varphi}{1 + [\omega\tau(1 - \beta\cos\theta)]^2}. \quad (15)$$

Then evaluating the integral of expression (15) in finite powers of $1/\omega\tau$, we have for the first and second terms,

predicted attenuation is why this process dominates the normal Landau-Rumer mechanism. In Al_2O_3 the ratio of the longitudinal velocity to the fast transverse velocity is approximately $\frac{5}{3}$.

Expression (41) can be fitted to de Klerk's data by using $\bar{A}_{s,t.,f.,t.,-f.,t.}^2(\text{noncollinear}) = \pm 3.6 \times 10^{12} \text{ dyne}^2/\text{cm}^2$.

C. Noncollinear Attenuation for $|\omega\tau(\beta-1)| > 1$

Finally, for completeness, we expand in the extreme non-energy-conserved limit. In this case, Eq. (16) becomes

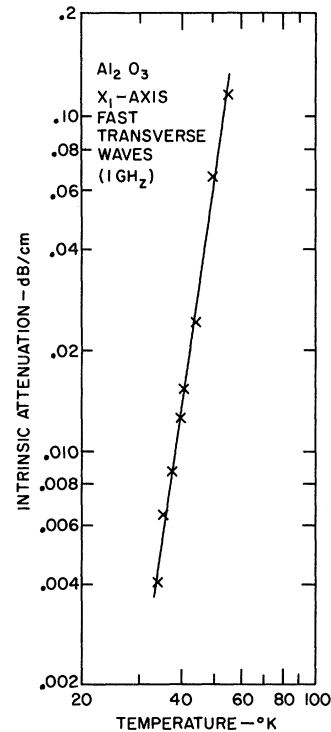


FIG. 6. Comparison of calculated attenuation (solid line) and the experimental values (\times) from de Klerk for the fast transverse wave in Al_2O_3 along the a axis.

$$\alpha = \frac{4 \cdot 34 \pi^2 \bar{h} \bar{A}^2 \cdot \text{i.t.} + \text{s.t.} - \text{s.t.} \cdot \text{(noncollinear)} \left(\frac{k_B T}{\bar{h}} \right)^4}{60 \rho^3 v^3 v_1^7} \times \frac{1}{\tau \beta^2} \left[\frac{4}{3} - \frac{8}{\beta^2} + \left(\frac{2}{\beta^3} - \frac{1}{\beta} \right) 2 \ln \left(\frac{1+\beta}{1-\beta} \right) \right].$$

This limit (as expected) has a simple T^4/τ temperature dependence.

V. CONCLUSION

The attenuation of transverse waves along the a axis in Al_2O_3 can be explained by taking into account two related factors. These are the lifetime of thermal phonons and the angular dependence of the coupling parameter. For the fast transverse wave the attenuation is dominated by interactions with thermal phonons of the same branch. The fact that the coupling parameter is zero for collinear interactions causes the allowed transitions to be zero. The attenuation was then dominated at lowest temperature by quasiallowed transitions and this ex-

plains the T^7 temperature dependence, i.e., lies between the T^4 and T^9 limits for allowed and unallowed processes.

The slow transverse wave is dominated by allowed processes with the fast transverse thermal phonons and has the expected T^4 dependence. The longitudinal wave is probably dominated by unallowed processes and has T^9 dependence.

This method can also be applied to the attenuation of transverse waves along any even-fold symmetry direction. For example, the measurements in the (110) direction LiF by de Klerk and Klemens,¹² or the slow transverse waves in X -cut quartz by Lewis and Patterson,¹³ or the (110) direction in InAs measured by Keck and Sladek.¹⁴ All these cases show temperature dependences somewhat like that of Al_2O_3 .

ACKNOWLEDGMENT

The authors wish to thank Dr. J. de Klerk for permission to reprint Fig. 2.

†This work partially supported by the Advanced Research Projects Agency.

*Present address: Department of Physics and Mathematics, Kentucky Wesleyan College, Owensboro, Ky. 42301.

¹R. Nava, R. Arzt, I. S. Ciccarello, and K. Dransfield, *Phys. Rev.* **134**, A581 (1964).

²S. Simons, *Proc. Phys. Soc. (London)* **82**, 401 (1963).

³L. Landau and G. Rumer, *Physik Z. Sowjetunion* **11**, 18 (1937).

⁴J. de Klerk, *Phys. Rev.* **139**, A1635 (1965).

⁵A. J. Leggett and D. ter Haar, *Phys. Rev.* **139**, A779 (1965).

⁶R. J. von Gutfeld and A. H. Nethercot, Jr., *Phys. Rev. Letters* **17**, 868 (1966).

⁷J. Kalejs, H. Maris, and R. Truell, *Phys. Letters* **23**, 299 (1966).

⁸H. J. Maris, *Phil. Mag.* **9**, 901 (1964).

⁹N. S. Shiren, *Phys. Letters* **20**, 10 (1966).

¹⁰R. E. Hankey and D. E. Schuele, *J. Acoust. Soc. Am.* **48**, 190 (1970).

¹¹R. C. Purdom, Ph.D. thesis (Purdue University, 1970) (unpublished).

¹²J. de Klerk and P. G. Klemens, *Phys. Rev.* **147**, 585 (1966).

¹³M. F. Lewis and E. Patterson, *Phys. Rev.* **159**, 703 (1967).

¹⁴M. J. Keck and R. J. Sladek, *Phys. Rev.* **185**, 1083 (1969).

Mixed-Mode Excitons in the Photoluminescence of Zinc Oxide—Reabsorption and Exciton Diffusion

R. L. Weiher and W. C. Tait

3M Company, St. Paul, Minnesota 55101

(Received 2 August 1971)

The photoluminescence of mixed-mode excitons in ZnO at 77 °K has been measured normal to the surface at various angles of the wave vector with respect to the \vec{c} axis. It is shown that the mixed-mode A ($n=1$) exciton-emission band is strongly influenced by reabsorption, and the exciton diffusion length is estimated to be 0.20 μ . The damping was found to be independent of the angle and was determined to be approximately $\hbar\Gamma=2.8$ meV.

I. INTRODUCTION

The existence of mixed-mode excitons¹ in the photoluminescence of uniaxial crystals has been previously verified.^{2,3} If the emission polarized

with the electric field \vec{E} in a plane containing both the photon propagation vector \vec{k} and the \vec{c} axis is measured with \vec{k} near $\vec{k} \perp \vec{c}$, as shown in Fig. 1(a), a narrow emission band is observed near the longitudinal exciton energy. As the angle between \vec{k} and